Energy Dependence of Proton Damage in Silicon*

G. W. SIMON, J. M. DENNEY, AND R. G. DOWNING
Space Technology Laboratories, Inc., Redondo Beach, California
(Received 5 November 1962)

The defect density in silicon resulting from proton bombardment has been caluclated from 10 MeV to 1.8 GeV. The results show that Rutherford scattering of the protons dominates defect production at low proton energies. Above 50 MeV, recoil nuclei resulting from spallation contribute significantly to the damage process. Good agreement between theory and experiments at 95.5 and 450 MeV is found, using the change in short circuit current density of solar cells and the change in minority carrier diffusion length as the experimental measures of lattice defects. The experimental results indicate that earlier theoretical models describing the slowing down of ions cannot satisfactorily explain the present observations.

I. INTRODUCTION

RADIATION damage experiments[1] at 450 MeV were previously proposed as evidence for the qualitative importance of spallation interactions to radiation damage at high proton energies. Following the early experiments, crude estimates[2] of the damage in silicon were made. These earlier reports and the discovery of high-energy protons in the trapped radiation belt have stimulated the more quantitative efforts described in this paper.

Radiation damage in crystalline solids is usually analyzed using elastic scattering theory. For low-energy charged particles, such as protons, the Mott–Rutherford cross section adequately describes the energy dependence of radiation damage. In this paper, we also consider the effects of initially inelastic interactions in contributing to the formation of lattice defects. The inelastic "spallation" products are analyzed with respect to the damage which they produce in silicon. The calculated defect density in silicon is then compared with the results of experiments at 95.5 and 450 MeV, using the change in short circuit current density and minority carrier diffusion length of solar cells as a measure of the lattice defects. These results quantitatively present the importance of the spallation mechanism in the production of lattice defects at high proton energies. The calculations have been carried out for silicon but can be expected to apply to other crystalline materials with appropriate changes in the numerical values; and, correspondingly, similar experimental behavior can be expected in other materials.

II. THEORY

Protons with energies greater than about 10 MeV which are scattered by silicon produce defects in the silicon lattice structure by two mechanisms: (a) elastic scattering and (b) inelastic collisions. In previous treatments of this problem (for example, see references 4, 5, and 11), the analyses have dealt exclusively with elastic collisions [mechanism (a)] between the incident proton and the primary "knock-on" atom which is displaced from its lattice site by this collision and with the subsequent defects produced in the lattice as this knock-on slows down through further collisions with other atoms. This approach has been satisfactory for the "low" proton energies (less than about 50 MeV) considered by these authors. However, at higher energies, inelastic nuclear collisions, which usually lead to spallation of the primary knock-on, become very important in the production of displacements. In this study, contrary to earlier approaches, we first briefly discuss elastic scattering but then mainly concentrate our analysis on the inelastic collision problem. In either process, we shall make the simplifying assumption that an atom is displaced from its lattice site whenever it receives kinetic energy greater than or equal to a so-called "minimum defect energy" E_d. We define a "defect density" ρ_d as the number of defects produced per cm^3 of target material/sec due to an incident flux of one proton/cm^2/sec:

$$\rho_d = N\sigma n, \tag{1}$$

where N = atomic density (atoms/cm^3) of the target material, σ = cross section for a defect-producing interaction, and n = number of defects per interaction. In terms of the two processes mentioned above, we write:

$$\rho_d = N(\sigma_e n_e + \sigma_i n_i) = \rho_e + \rho_i, \tag{2}$$

where the subscript e refers to elastic and i to inelastic interactions.

In the following two sections, we calculate first the number of displacements due to elastic collisions and then those due to spallation of the target nucleus. The elastic calculation (Sec. A, following) is straightforward, using classical Rutherford scattering theory. However, the inelastic collision theory described in Sec. B involves several uncertainties, which are discussed both in Sec. C and Part IV.

A. Elastic Scattering

At the proton energies being considered, the proton effectively penetrates the electron cloud and interacts with essentially an unscreened silicon nucleus via Coulomb repulsion, that is, by Rutherford scattering.

* This research was supported by the National Aeronautics and Space Administration, Goddard Space Flight Center.
[1] R. Smoluchowski, Phys. Rev. **94**, 1409 (1954); E. Pearlstein, H. Ingham, and R. Smoluchowski, *ibid.* **98**, 1530 (1955).
[2] J. M. Denney and D. Pomeroy, Proc. Inst. Radio Engrs. **48**, 950 (1960).

Since we are concerned here only with those collisions which displace an atom from its lattice position, we are interested in the integrated Mott–Rutherford cross section for interactions involving energy transfers greater than E_d to the recoil nucleus. This is given by[3,4]

$$\sigma_e=(\pi b^2/4\gamma^2)[(\epsilon-1)-\beta^2\ln\epsilon+\pi\alpha\beta\{2(\epsilon^{1/2}-1)-\ln\epsilon\}], \tag{3}$$

where $\gamma=(1-\beta^2)^{-1/2}$, $\beta=v/c$, $b=2Z_2e^2/(mc^2)\beta^2$, $\epsilon=E_m/E_d$, $\alpha=Z_2e^2/\hbar c$, and $E_m=2E(E+2mc^2)/[(1+m/M)^2(Mc^2)+2E]$. In these relations, m, v, and E refer to the proton mass, velocity, and energy; M and Z_2 to the silicon mass and charge number; and E_m is the maximum possible energy transfer to the silicon nucleus. The average energy transferred to the knock-on in these interactions is

$$\bar{E}=E_d[\ln\epsilon-\beta^2+\pi\alpha\beta], \tag{4}$$

whenever $\epsilon\gg1$ as in the present study.

Because of its logarithmic dependence on E, the energy $\bar{E}$ is quite insensitive to the incident proton energy E, and varies from 100 to 200 eV for proton energies between 10 and 1800 MeV, the energy range investigated in this paper. As the primary knock-on of average energy $\bar{E}$ is brought to rest by elastic collisions with other lattice atoms, it produces secondary, tertiary, etc., defects in the lattice. It has been shown by a number of authors[5,6] that in elastic collisions about half of the initial energy goes into defect production, so that the total number of defects n_e is approximately

$$n_e\approx\tfrac{1}{2}(\bar{E}/E_d). \tag{5}$$

Combining (3), (4), and (5) yields the elastic contribution to the defect density (2):

$$\rho_e\simeq(\pi b^2N\epsilon/8\gamma^2)[\ln\epsilon-\beta^2+\pi\alpha\beta], \tag{6}$$

in which we have used the fact that all terms except the first in the square brackets in (3) are negligible relative to ϵ.

It should be noted that at nonrelativistic proton energies, Eq. (6) reduces to the simple form

$$\rho_e(E)=(C_0/E)(C_1+\ln E), \tag{6a}$$

where C_0 and C_1 are constants.

B. Inelastic Scattering

Inelastic interactions produce few defects relative to those from Rutherford scattering for proton energies below about 50 MeV. However, at higher energies, the inelastic contribution becomes the dominant defect-producing mechanism. Spallation of the target nucleus is the primary result of these inelastic interactions.

Following Serber,[7] the spallation process can be considered to be comprised of two parts. In the first, or cascade portion of the interaction, the incoming proton collides with individual nucleons in the target nucleus. These collisions result[8] in the ejection of a few fast nucleons, which have a roughly $E^{-1/2}$ energy distribution from about 5 MeV up to the energy of the incident proton and are emitted primarily in the direction of the incident proton. In addition, the residual nucleus recoils with an average energy which is approximately linearly proportional to that of the incident proton.[9] In the second stage, the residual nucleus, which has been left in an excited state by the cascade process, evaporates a number of nucleons with average energy of 10 to 15 MeV.[10]

We shall ignore the gamma rays and pions which are, of course, emitted in these processes, since their contribution to defect production is negligible. It should also be noted that some of the processes described in this section involve elastic scattering but have been considered here as "inelastic" processes, since they result from a primary event (spallation) which is inelastic.

The defect density due to inelastic scattering can then be written

$$\rho_i=N\sigma_i[n_{\mathrm{RN}}+(mpn)_{\mathrm{FP}}+(mpn)_{\mathrm{FN}}+(mpn)_{\mathrm{SP}}+(mpn)_{\mathrm{SN}}], \tag{7}$$

where the subscripts mean: RN = recoil nucleus, FP and FN = fast proton and neutron (from cascade), and SP and SN = slow proton and neutron (from evaporation), while m = number of nucleons of each type emitted per inelastic interaction and p = geometric probability factor that the emitted particle will interact before leaving the particular sample of silicon in question.

Calculation of the quantity p is as follows: $p=Nx\sigma$, where N = atomic density, x = path length the particle travels in the target material, and σ is the cross section for a defect-producing interaction. For both fast and slow neutrons, an average cross section of one barn was assumed. In the case of protons, since their energies lie mainly below 100 MeV, elastic scattering was considered to be the principal displacement mechanism. Thus, an average, or effective, Rutherford cross section was calculated from the energy distributions of the emitted protons. These assumed distributions were $\Phi(E)=\Phi_0/E^{1/2}$ for the fast protons and $\Phi(E)=\Phi_0(E-E_0)e^{-C(E-E_0)}$ for the slow protons, as obtained from references 8 and 10, respectively. For the silicon samples investigated, the distance x was 2 mils for the fast particles and 8 mils for

[3] N. Bohr, Kgl. Danske Videnskab. Selskab. Mat.-Fys. Medd. **18**, No. 8 (1948).
[4] F. Seitz and J. S. Koehler, in *Solid State Physics*, edited by F. Seitz and D. Turnbull (Academic Press Inc., New York, 1956), Vol. 2, p. 305.
[5] G. H. Kinchin and R. S. Pease, in *Reports on Progress in Physics* (The Physical Society, London, 1955), Vol. 18, p. 1.
[6] W. S. Snyder and J. Neufeld, Phys. Rev. **97**, 1636 (1955).
[7] R. Serber, Phys. Rev. **72**, 1114 (1947).
[8] N. Metropolis, R. Bivins, M. Storm *et al.*, Phys. Rev. **110**, 185 and 204 (1958).
[9] N. T. Porile, Phys. Rev. **120**, 572 (1960).
[10] K. J. LeCouteur, Proc. Phys. Soc. (London) **A63**, 259 (1950).

the slow particles, since the latter are emitted isotropically and, thus, have a longer average path length in the slab geometry considered. These dimensions are representative of photovoltaic devices; the results are relatively insensitive to the actual values chosen.

The number of defects, n, per interaction was calculated as described in the section on elastic scattering, while the cross section σ_i and the number of emitted fast nucleons m_{FP} and m_{FN} were obtained from Metropolis.[8] Metropolis also gave the average excitation energy of the residual nucleus, from which it was possible to estimate the numbers, m_{SP} and m_{SN}, of slow particles emitted in the evaporation stage.

For the geometry studied, it was found that the total contribution to the defect density from both cascade and evaporated nucleons, at all energies, was not more than about 1% of that due to the recoil of the residual nucleus. We have neglected in this paper the emission of particles with $A>1$, although one would expect perhaps 1/5 to 1/3 of the cascade and evaporated particles to fall in this category. The small difference in defect production between $A=1$ and $A>1$ particles is not important here, since the contribution of the emitted particles is such a small percentage of the total defect production.

It should be noted that the calculation of the geometrical probability factor p has assumed that the distance x is much smaller than the range R of the particle in the target material. That is, we have assumed that the particle's energy and direction remain essentially unchanged during the one or several scatterings which occur before it escapes from the target. These assumptions are valid for the solar cells studied. In the case of thick targets (x of the order of R), the expression (mpn) of (7) must be replaced by (mn), where n is now defined as $n=\frac{1}{2}(\nu/E_d)$. (The quantity ν is defined in the next paragraph.) For such targets, the displacements due to the emitted nucleons may outnumber those from the recoiling nucleus; and then the emission of some heavier-than-nucleon particles must be taken into account.

In our case, it is of primary importance to understand well the behavior of the recoil nucleus as it slows to rest. This complex problem has been the subject of many investigations during the past two decades and can be outlined as follows: The recoiling nucleus, initially having a kinetic energy of a few MeV, at first slows down primarily by ionizing inelastic collisions with the electrons of the lattice atoms. This process does not contribute to the number of atomic displacements in the lattice. As it continues to slow down, the moving ion begins to lose more of its energy in elastic defect-producing collisions with the lattice atoms themselves, and less in electron interactions. Some authors[5,6,11] have defined a critical energy E_i below which all collisions are assumed to be elastic and above which almost all the interactions are inelastic. In this paper, we use the results of Lindhard, Scharff, and Thomsen[12,13] who do not invoke a cutoff energy E_i but instead define an electronic stopping cross section proportional to the velocity of the moving ion and a nuclear stopping cross section derived from an approximate Thomas–Fermi potential function. These cross sections, assumed to be valid over the entire energy range of interest, are inserted into the integral equations which describe the slowing-down process, and the equations are solved numerically. Results are given in terms of the energies $\nu(E)$ and $\eta(E)$ which go into elastic and inelastic collisions, respectively, if the recoil nucleus initially has energy E, i.e., $E=\nu+\eta$. The number of defects, n_{RN}, in (7) is then given approximately by application of (5):

$$n_{RN}=\tfrac{1}{2}\nu/E_d. \tag{8}$$

The numerical results presented by Lindhard[12] are valid only for $Z_1=Z_2$, where the subscripts refer to the incident and target particles, respectively. In our case, the recoiling ion has lost a number of nucleons in the cascade and evaporation processes and, thus, $Z_1<Z_2$, $A_1<A_2$. Lindhard and Nielsen[14] have helped us greatly by making a series of special calculations for a Si target ($Z_2=14$, $A_2=28$) and various incident particles. Their results are shown in Fig. 1. As would be expected, the elastic energy loss (ν) increases as Z_1 and A_1 increase.

C. Results of the Calculations and Sources of Error

Results of the theoretical calculations are shown in Fig. 2. The elastic scattering clearly dominates below 50 MeV, while the spallation interaction is of primary importance above 200 MeV.

Errors, due to the theoretical models used, may change the absolute magnitude of the calculated defect density. However, no significant change is expected in the *shape* of the ρ versus E_p curve, which is the primary thing being compared with experiment in this study. Possible errors in the theoretical calculations include the following:

Results of the Monte Carlo calculations[8] are to be considered in "semiquantitative" agreement with experiment, according to the authors. In addition, we have made additional extrapolations from these results, which may cause other small errors: The recoil momentum of the residual nucleus (Si^{28} minus prongs) was estimated from Porile's calculations[9] for Ru^{100} and U^{238}. Values of the recoil momentum for $E_p<80$ MeV were extrapolated from the Monte Carlo data which only considered $E_p\geq 80$ MeV. Errors in ρ_t from this cause are very minor, since $\rho_e\gg\rho_i$ in this energy region. Another negligible error comes from using the Monte Carlo results for Al^{27} to describe the behavior of Si^{28}.

[11] F. Seitz, Discussions Faraday Soc. 5, 271 (1949).

[12] J. Lindhard, M. Scharff, and P. V. Thomsen (1961, unpublished).

[13] J. Lindhard and M. Scharff, Phys. Rev. 124, 128 (1961).

[14] J. Lindhard and Mrs. V. Nielsen (private communication).

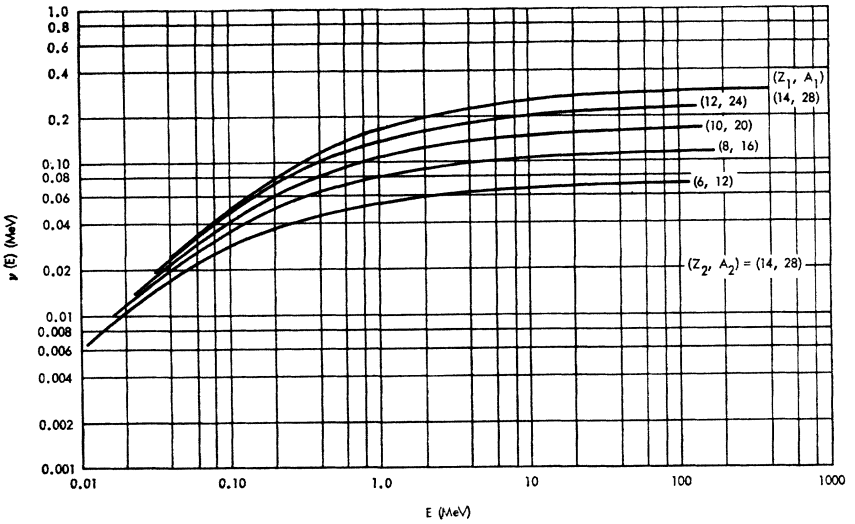

FIG. 1. Amount of energy (ν) lost in elastic collisions by a particle (Z_1,A_1) in slowing to rest from an initial energy E. The target material (Z_2,A_2) is Si. Data are courtesy of J. Lindhard and V. Nielsen (unpublished).

Two errors in the Lindhard[12] model may cause minor changes in our results: (a) The authors point out that the Thomas–Fermi potential functions used may give values of $\nu(E)$ about 10% high at high energies. (b) They have neglected the energy loss E_d in elastic collisions, which would also reduce $\nu(E)$ somewhat.

III. EXPERIMENTAL RESULTS

Radiation damage experiments have been conducted at proton energies of 20.5, 95.5, 400, 450, and 740 MeV. The details and results of these experiments are described elsewhere.[15] The experiments consisted primarily of exposing silicon solar cells to the external proton beam of a cyclotron. Flux measurements were obtained by standard procedures which employed the use of secondary emission monitors, ionization chambers, C^{11} activation, film densitometry, and Faraday cups. All of the experiments and associated measurements were conducted at room temperature. Experimental parameters investigated consisted of measurements of I–V characteristics and short circuit current under illumination, spectral response, and minority carrier diffusion lengths. All of these electrical measurements could be performed with a greater degree of accuracy than the proton flux determinations. Thus, the limiting accuracy in all of the experiments is the accuracy with which flux determinations were obtained.

The choice of silicon solar cells as experimental test specimens serves a double purpose. First, the electrical performance of solar cells is directly related to bulk minority carrier lifetime which, in turn, is the most sensitive parameter to the presence of lattice defects. Secondly, silicon solar cells serve as the primary source of electrical power in most contemporary spacecraft systems, thus rendering experimental data of immediate practical importance.

One can make a large number of interesting electrical measurements which concern the effect of proton radiation on silicon solar cell operation. Several of these measurements, i.e., I–V, maximum power, and efficiency, are of primary importance to satellite power supply system design. Since the primary effect of radiation on silicon is the reduction of minority carrier lifetime in the bulk material, other electrical parameters such as short circuit current density and minority carrier diffusion length are of primary importance in determining the radiation sensitivity of silicon solar cells. Thus, in the experiments referenced above, considerable attention was given to the measurement of the short-circuit current density, J_{sc}, minority carrier diffusion length, L, and the damage effectiveness constant, K which is derived from L.

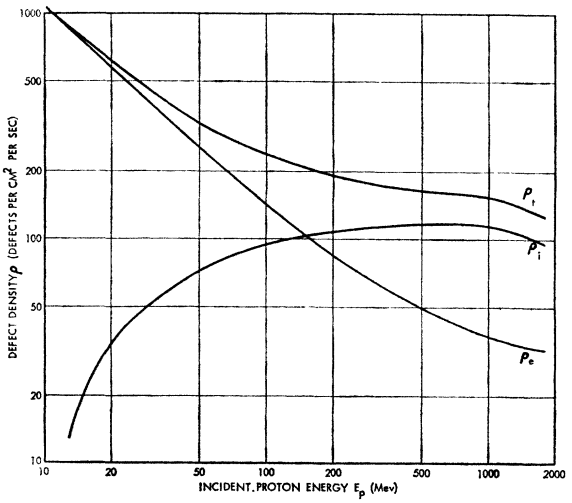

FIG. 2. Theoretical defect density (ρ) in Si due to elastic (ρ_e) and inelastic (ρ_i) collisions as a function of incident proton energy E_p.

[15] J. M. Denney and R. G. Downing, Final Report, National Aeronautics and Space Administration Contract NAS5–613, 15 September 1961 (unpublished).

In all of the experiments, J_{sc} and J_{sc}/J_{sc_0} were obtained with 2800°K tungsten light. The advantages in using 2800°K tungsten light lie in its ease of reproducibility and in its high red component which tends to amplify the radiation damage in the bulk material and minimize differences in cell surface characteristics. A common technique for expressing radiation sensitivity is to express an integrated flux, Φ_c, required to produce a given amount of degradation in either J_{sc} or J_{sc}/J_{sc_0}. It has been shown that the rate of degradation in short-circuit current density for silicon cells is a constant independent of irradiating particle type or energy. This is due to the optical absorption characteristics of light in silicon. For 2800°K illumination, the degradation rate has been shown to be about 25% per decade of integrated flux for a J_{sc}/J_{sc_0} analysis or about 6 ma/cm^2-decade for a J_{sc} analysis.

The advantage in analyzing radiation damage using J_{sc} is that, for cells having different initial diffusion lengths and correspondingly different initial J_{sc}'s but similar surface characteristics, the data yield significant values of Φ_c. However, if the surface characteristics of different types of cells are far different, the results of a J_{sc} analysis will lead to erroneous energy dependence comparisons of Φ_c. On the other hand, the use of a J_{sc}/J_{sc_0} comparison quite capably handles the large range of differences of surface characteristics of different types of solar cells, but only cells having very nearly identical initial diffusion lengths and corresponding short-circuit currents can be compared on this basis. It is clear then that neither of these two types of analyses is sufficient for comparing all of the existing data obtained on different types of cells under varying experimental conditions over a long period of time.

A more direct and quantitative measure of radiation damage in silicon can be obtained through measurements of the minority carrier diffusion length, since the introduction of lattice defects in silicon produces a decrease in minority carrier lifetime as one of the most sensitive consequences. After the initial defect concentration is exceeded in a radiation damage experiment, the minority carrier lifetime decreases as:

$$1/\tau = 1/\tau_0 + K'(E_p)\Phi, \tag{9}$$

where τ_0 and τ are the initial and final minority carrier lifetime, respectively, K' is the damage effectiveness coefficient, K, times the minority carrier diffusion coefficient, and Φ is the integrated proton flux.

Converting Eq. (9) to minority carrier diffusion length yields

$$1/L^2 = 1/L_0^2 + [K'(E_p)/D]\Phi, \tag{10}$$

where L_0 and L are initial and final minority carrier diffusion lengths, respectively, and D is the minority carrier diffusion coefficient. The derivative is a measure of the defect introduction rate

$$d(1/L^2)/d\Phi = K'(E_p)/D = K(E_p). \tag{11}$$

Neglecting annealing and differences in local defect densities, Eq. (11) provides another basis for experimentally determining the energy dependence of the proton damage. It has been shown,[16] however, that for high-energy proton bombardment the L and corresponding K for a given cell is not constant but actually dependent upon the minority carrier densities at the time of measurement. It is important, then, when attempting to assign a K value to a given proton energy, that the proper value of K be used for the comparisons which are made. Here, the K values used are those for an incident illumination intensity of one sun. In this way, the energy dependence of the K value can be compared to the Φ_c's obtained using a J_{sc} and a J_{sc}/J_{sc_0} analysis.

The analysis of the experimental data for comparison with the theoretical curve presented in Fig. 2 is restricted here to the two experiments possessing the highest degree of accuracy in the determination of the proton integrated flux. These were the experiments conducted at 450 and 95.5 MeV which are considered to be accurate to within 5%. Due to the rapid advancement in the "state of the art" of silicon solar cells and the long time span, in excess of a year, covered by these experiments, accurate energy comparisons are not possible on all of the different types of cells tested in these experiments. To insure maximum confidence in the comparison of the data at these various energies, therefore, it was required that all of the three analysis techniques discussed above yield similar energy dependences. Since it is the primary purpose of this paper to compare energy dependence, and not the absolute magnitude of the damage rates, only the ratios of the K

TABLE I. Comparison of experimental and theoretical energy dependence.

	ρ_e(95.5 MeV)/ρ_e(450 MeV)	ρ_i(95.5 MeV)/ρ_i(450 MeV)	K(95.5 MeV)/K(450 MeV) for one sun illumination	Φ_c(95.5 MeV)/Φ_c(450 MeV) for J_{sc}=19 mA/cm^2	Φ_c(95.5 MeV)/Φ_c(450 MeV) for J_{sc}/J_{sc_0}=0.75
Ratio	2.85	1.48	2.35	2.40	2.20

[16] J. M. Denney, R. G. Downing, and G. W. Simon, ARS Space Power Systems Conference, 25–28 September 1962, Rept. No. 2536–62 (unpublished).

values and the Φ_c's will be presented here. Using standard commercially available p on n solar cells, the ratios of the damage constants are given in Table I and compared with the ratios that would be expected from both the ρ_t and the ρ_e curves.

IV. DISCUSSION

The most significant result of the calculations is that the defect production for E_p greater than about 150 MeV is dominated by "inelastic" processes. This conclusion is based upon Monte Carlo calculations[8] and a theoretical model developed by Lindhard *et al.*[12,14,17] The major uncertainty in the analysis is the use of an average momentum for the recoil nucleus instead of employing a momentum distribution. Nevertheless, the results shown in Fig. 2 are expected to be qualitatively correct, in shape if not in absolute magnitude.

In Sec. II we have computed the total number of defects resulting from atomic displacement on a one-for-one basis. We have neglected both the local distribution of these defects and defect annealing in comparing the calculated values and the experimental measurements. The defects produced by the recoil nucleus occur in small "clumps" because of the very short range of the recoiling residual nucleus, while low-energy protons are expected to produce a more homogeneous distribution of defects. This variation in local defect densities influences the experimental measurements as well as the thermal recombination rate of the defects. Therefore, the calculated defect density tends to over estimate the actual number of defects produced, particularly for the "clumps" formed by the recoil nuclei. For these reasons and because there is no satisfactory functional relationship between electrical properties and the number of lattice defects, a satisfactory comparison between experimental data and the calculated curves is difficult. Despite these limitations, a comparison has been made (Sec. III) which indicates that the inelastic contribution cannot be neglected. The experimental measurements, regardless of the method, demonstrate an energy dependence lying between the "ρ_e" and "ρ_i" curves of Fig. 2. Because the elastic and inelastic contributions are essentially independent and because of the over estimate of defect effectiveness in the "clumps" in comparing the experiments with the "ρ_i" curve, the experimental results appear to be consistent with the theory.

The use of a sharp threshold, E_i, in the recoil nucleus damage calculations fails by a considerable margin to provide agreement with the experimental results. That is, either E_i must be unreasonably assumed to be about 250 keV in order to achieve quantitative agreement, or E_i is taken as 10 keV and then unreasonable conclusions regarding the carrier-trapping cross section of the recoil nucleus damage are required. For these reasons, in addition to those given by Lindhard, Scharff, and Thomsen, we conclude that the sharp-threshold approximation, E_i, is inappropriate for the recoil damage calculations.

When further experimental evidence is available, the shape of the defect density versus energy curve should provide additional information in several areas of interest. For example, if we assume the correctness of the low-energy elastic scattering model, then the shape of the total defect density yields the inelastic contribution to the number of defects and gives information concerning the efficiency of the recoiling nuclei in changing the minority-carrier diffusion length, i.e., the relative importance of uniformly distributed defects versus clumps of defects.

It should be noted that the ρ_i versus E_p curve (Fig. 2) levels off at a proton energy of about 300 MeV and then starts to decrease near 1 GeV. This occurs despite the increasing momentum of the recoiling ion with increasing E_p. The higher the incident proton energy the more nucleons are lost by the struck nucleus and, thus, the smaller the charge and mass of the residual ion, with resulting decrease in ν (Fig. 1). Thus, at very high energies, the ρ_t vs E_p curve should depend on the relative importance of the recoil nucleus compared to the emitted nucleons in producing defects. If the recoil nucleus dominates, the curve will follow the form of Fig. 2 and drop off at high energies, while if the nucleons are of primary importance, the shape continues to rise as the number of nucleons is roughly proportional to the incident proton energy. Information regarding this phenomenon would require thicker targets than studied here to increase the nucleon contribution.

The theory and the comparative experiments described in this paper suggest a number of additional interesting topics. For example, the recombination and trapping centers associated with the defect clumps produced by the recoil nuclei can be expected to be different from those associated with isolated point defects. Also, very little consideration has been given to any descriptive detail of these clumps and their effect on the surrounding lattice. Recent experiments[16] suggest that the recombination centers associated with the defect clumps are sensitive to the minority carrier concentration in silicon in contrast to recombination centers produced by electron bombardment. These and other related problems are being investigated by research now in progress, which should also help to resolve the practical proton energy dependence of damage in photovoltaic devices.

ACKNOWLEDGMENTS

We gratefully acknowledge the assistance of many co-workers. In particular, we are indebted to J. Lindhard and Mrs. V. Nielsen for special calculations made for us, and to J. Lindhard, M. Scharff, and P. V. Thomsen for valuable correspondence and permission to quote their unpublished calculations.

[17] J. Lindhard and P. V. Thomsen, Symposium on Radiation Damage, Venice, May 1962 (unpublished).